Analyst

ARTICLE

Received 00th January 20xx,

Accepted 00th January 20xx

DOI: 10.1039/x0xx00000x

www.rsc.org/

Monoclonal antibody-based immunosensor for the electrochemical detection of imidacloprid pesticide

Beatriz Pérez-Fernández [a], Josep V. Mercader [b], Brenda I. Checa-Orrego [c], Alfredo de la Escosura-Muñiz *[a] and Agustín Costa-García *[a]

Imidacloprid (IMD) is one of the most used pesticides worldwide, as systemic insecticide as well as for pest control and seed treatment. The toxic and potential carcinogenic character of IMD makes its monitoring of great relevance in the field of agriculture and environment, so sensitive methodologies for in field analysis are strongly required. In this context, we have developed a competitive immunoassay for the determination of IMD using specific monoclonal antibodies followed by electrochemical detection on screen-printed carbon electrodes (SPCE). The optimized immunosensor exhibited a good reproducibility (RSD of 9%) and a logarithmic response in the range 50 – 10000 pM of IMD, with an estimated detection limit (LOD) of 24 pM, which was below the maximum levels allowed by the legislation. High-Performance Liquid Chromatography-Mass Spectrometry-Mass Spectrometry (HPLC-MSMS) and Enzyme-Linked Immunosorbent Assay (ELISA) analysis were also performed for comparison purposes, where the electrochemical immunosensor exhibited wider range of response and lower detection limit. Matrix effects below 6.5% were obtained using tap water samples. All these characteristics make our electrochemical immunosensor as a valid and advantageous method for the *in field* determination of IMD.

1 Introduction

Neonicotinoid insecticides are a type of pesticides that act on the nicotinic acetylcholine receptor (nAChRs) in the central nervous system of insects, causing paralysis and death [1,2]. Imidacloprid (N-[1-[(6-chloropyrid-3-yl) methyl]-4,5-dihydro-1H-imidazol-2-yl] nitroamide) (IMD) is a neuroactive insecticide derived from nicotine used as systemic insecticide and for pest control and seed treatment. However, it also acts on insects beneficial to the environment such as bees. As a result, IMD is the cause of a syndrome called Colony Collapse Disorder (CCD), which symptoms are related to the presence in the abandoned colony of i) bee offspring, ii) stored food (honey and pollen) and iii) the queen bee. This represents a critical environmental problem that leads to a decline in pollination leading to a decrease in the production of food for human beings [3,4].

Currently, IMD is categorized as moderately toxic by the World Health Organization (WHO) and the United States Environmental Protection Agency (USEPA) (class II or III, which requires “Hazard” or “Caution” label) [5]. It is also classified as a “probable” carcinogen by the Environmental Protection Agency (EPA) [6]. The determination is of great relevance in the field of agriculture and environment [7], and thus it is important to develop devices that can be used at the point-of-use. This insecticide has a prolonged residual effect in soils, so it can be found in fruits, vegetables and water samples. In surface water it is degraded in a series of toxic compounds for vertebrates, mammals and humans, due to the action of atmospheric parameters such as sunlight, pH, temperature, etc. The maximum residual limit (MRL) in the European Union is 0.5 µg L^{-1} for total pesticides and 0.1 µg L^{-1} for the individual pesticides [8]. This means that so very sensitive techniques are needed for detecting IMD at trace levels.

Normally, insecticides are determined by chromatographic techniques, such as High-Performance Liquid Chromatography (HPLC), HPLC-Mass Spectrometry-Mass Spectrometry (HPLC-MSMS) or Gas Chromatographic-MSMS (GC-MSMS) [9–12], in addition to Enzyme-Linked Immunosorbent Assay (ELISA) [13–15]. Chromatographic techniques have inherent drawbacks related to their time-consuming procedures, complex pre-treatment of samples, high cost of instruments and the need of specialized personnel. Electrochemical sensors have emerged in recent years as alternatives for pesticides detection, with benefits related to the low cost, simplicity, high sensitivity and waste reduction, among others [16,17]. The redox properties of IMD and other pesticides allow their detection through electrochemical measurements [18–20]. However, the determination by immunosensors has advantages over the redox detection mostly due to the high selectivity given by specific antibodies.

In this context, we propose here a novel immunosensor for the electrochemical determination of IMD on screen-printed carbon electrodes (SPCEs), taking advantage of the properties described above. The indirect detection through a competitive immunoassay

[a] Department of Physical and Analytical Chemistry, University of Oviedo, Julián Clavería 8, 33006, Oviedo, Spain. E-mail address: alfredo.escosura@uniovi.es; costa@uniovi.es
[b] IATA-CSIC, Avda Agustí Escardino 7, 46980, Paterna (Valencia), Spain.
[c] Ministerio de Desarrollo Agropecuario DNSV, Panamá.

presents important advantages over the direct electrochemical detection in terms of selectivity and sensitivity. Advantage is taken of the use of novel monoclonal antibodies [21] which allow improvement of such parameters as well as the advantages of the SPCE electrodes in terms of small size, disposability, low cost and ease of surface modification [22].

Fig. 1 Scheme of the indirect competitive immunosensor for the detection of IMD on SPCEs using monoclonal antibodies.

2 Materials and methods

2.1 Apparatus and electrodes

Chronoamperometric measurements were performed with a potentiostat/galvanostat μAutolab Type II purchased from Eco-chemie (The Netherlands) controlled by GPES 4.9 software. All measurements were carried out at room temperature. Screen-printed carbon electrodes (SPCEs) (carbon working and counter electrodes and silver/silver chloride quasi-reference electrode) (ref. DRP-110) and the connector to the potentiostat (ref. DRP-DSC) were purchased from Dropsens (Spain).

HPLC-MSMS experiments for the determination of IMD were carried out using a liquid chromatograph model 1260 Infinity from Agilent (Germany) coupled to a triple quadrupole mass spectrometer model 6460 also from Agilent (Germany). The mobile phases were (A) water/methanol (80:20) with 5 mM ammonium acetate and (B) acetonitrile with 5 mM ammonium acetate.

2.2 Reagents and solutions

Imidacloprid PESTANAL®, analytical standard, Phosphate buffered saline (PBS) 10 mM pH 7.4, Bovine Serum Albumin fraction V (BSA), 3,3',5,5' tetramethylbenzidine (TMB), Glyphosate PESTANAL®, Parathion PESTANAL®, Thiamethoxam PESTANAL® and Carbendazim PESTANAL®, were purchased from Sigma-Aldrich (Spain). Permethrin was provided by LGC Standars. Antigen-protein conjugate (BSA-IMD) and anti-IMD monoclonal antibody (mAb-IMD) were provided by University of Valencia and IATA-CSIC Valencia (Spain). Polyclonal rabbit anti-mouse IgG-HRP (anti-IgG-HRP) was purchased from Dako, Agilent (Spain). Ultrapure water obtained with an EMD Millipore™ Direct-Q5™ purification system from Millipore Ibérica SA. (Spain) was used throughout this work. All chemicals employed were of analytical reagent grade. Working solutions of BSA-IMD, mAb-IMD, anti-IgG-HRP, BSA were prepared daily in 10 mM pH 7.4 PBS buffer. An ELISA kit for IMD detection (ref. PN500800) was purchased from Abraxis (USA).

2.3 Immunoassay procedure

2.3.1 Immunosensor preparation. 10 μL of 0.5 μg mL^{-1} BSA-IMD solution in 10 mM PBS (pH 7.4) were dropped on the surface of the working electrode and incubated at 4ºC overnight. After washing with water, 40 μL of 1% BSA in PBS 10 mM (pH 7.4) were dropped and left there for 40 min, before washing. Then, 10 μL of a mixture of 0.8 μL mL^{-1} mAb-IMD and different concentrations of free IMD in 10 mM PBS (pH 7.4) with 0.5% BSA were dropped on the modified electrodes and left there for 1h. After washing with water, 10 μL of 1 μg mL^{-1} anti-IgG-HRP in 10mM PBS (pH 7.4) with 0.5% BSA were added and incubated for 1h, before finally washing with water.

2.3.2 Electrochemical detection. The enzymatic reaction was carried out by placing 40 μL of TMB solution and incubating for 1 min. Chronoamperometric detection was performed applying a constant potential of -0.2 V during 60 s and recording the current associated with the TMB reduction process [23,24]. The analytical signal was the absolute value of the current recorded at 60 s. All measurements were done in triplicate.

The signal to noise ratio (S/N) was chosen as the analytical parameter for the optimization of the experimental conditions of the immunosensor shown at *section 3.1.*

2.3.3 Tap water sample preparation and analysis. Tap water was doped with 500 pM and 1000 pM solutions of IMD. The samples were analysed in triplicate following the above detailed electrochemical method.

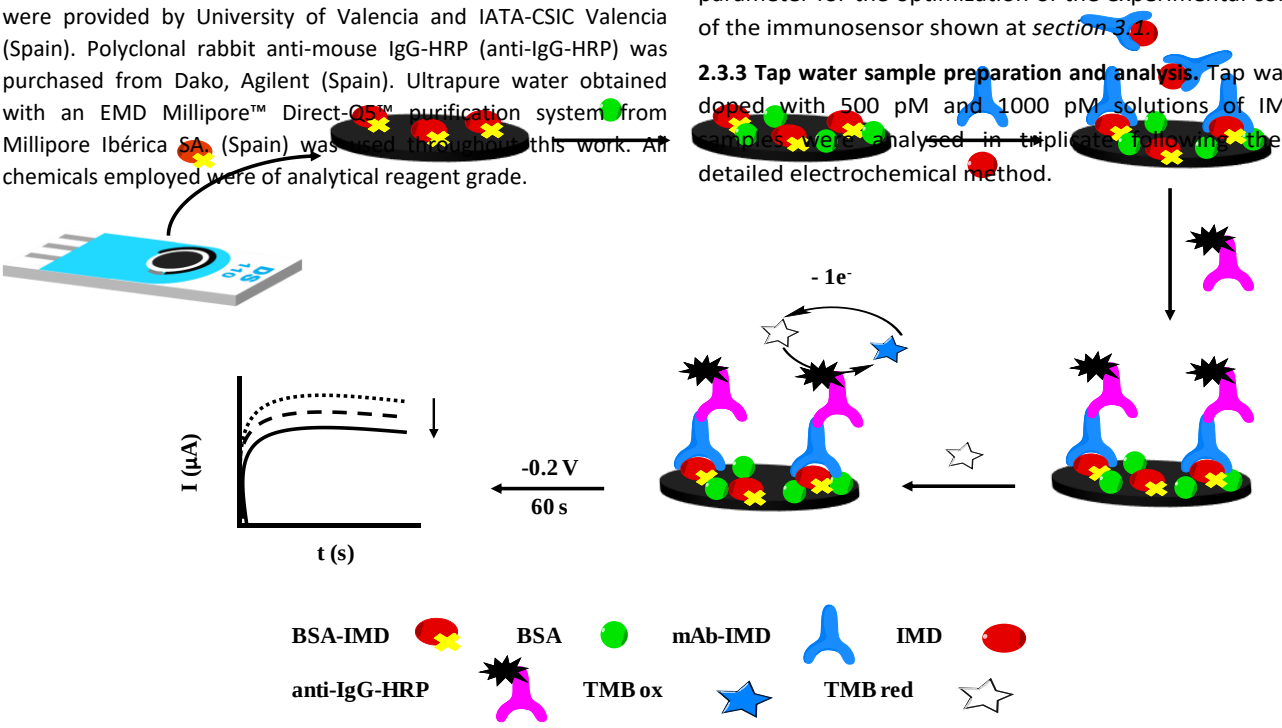

IMD was also determined by HPLC-MSMS and ELISA for comparison purposes. The detailed experimental procedures are described at the electronic supplementary information.

3 Results and discussion

3.1 Sensing principle: indirect competitive immunoassay using monoclonal antibodies

The scheme of the competitive immunoassay is shown in Figure 1. BSA-labelled antigen (BSA-IMD) immobilized on the SPCE surface and free IMD analyte compete for the specific mAb-IMD monoclonal antibody. HRP label is specifically linked to the electrode through anti-IgG-HRP secondary antibodies. After that, the added TMB reagent is enzymatically oxidized by the HRP molecules. The oxidized TMB is reduced back at the surface of the SPCE by applying a constant potential of -0.2 V during 60 seconds, producing an associated catalytic current (analytical signal) that is proportional to the IMD amount[23,24].

3.2 Optimization of experimental conditions

3.2.1 BSA-IMD concentration. To evaluate the optimum concentration of the BSA-labelled antigen immobilized on the electrode, BSA-IMD from different solutions (from 0 to 5 µg mL^{-1}) was immobilized on the electrode (overnight at 4°C). mAb-IMD and anti-IgG-HRP concentration were fixed at 2 and 5 µg mL^{-1} respectively (1h of reaction for both of them). In Figure 2A it can be observed that the signal to noise (S/N) ratio increases with the BSA-IMD concentration, reaching saturation of the electrode for 0.5 µg mL^{-1}. Thus, that concentration was selected as optimum for the immunosensor development.

3.2.2 mAb-IMD concentration. A key parameter in the development of the competitive immunoassay is the concentration of the monoclonal antibody specific against the free analyte (mAb-IMD). Different concentrations of mAb-IMD in the range 0 to 1 µg mL^{-1} were evaluated, fixing the BSA-IMD at 0.5 µg mL^{-1} and anti-IgG-HRP at 5 µg mL^{-1}. As shown in Figure 2B, the minimum concentration of monoclonal antibody giving the maximum S/N ratio corresponds to 0.8 µg mL^{-1}, this value was chosen as optimum for the competitive assay.

3.2.3 Anti-IgG-HRP concentration. The last parameter optimized was the concentration of anti-IgG-HRP used in the final enzymatic reaction for revealing the immunoassay. Different concentrations were evaluated (0 to 6 µg mL^{-1}; 1h of incubation), while fixing the rest of parameters at the optimum levels. In Figure 2C it can be seen a high increase in the S/N ratio for concentrations up to 3 µg mL^{-1}. A slight increase of S/N ratio with a clear saturation was noticed for higher concentrations, so 3 µg mL^{-1} was selected as optimum for revealing the immunoassay.

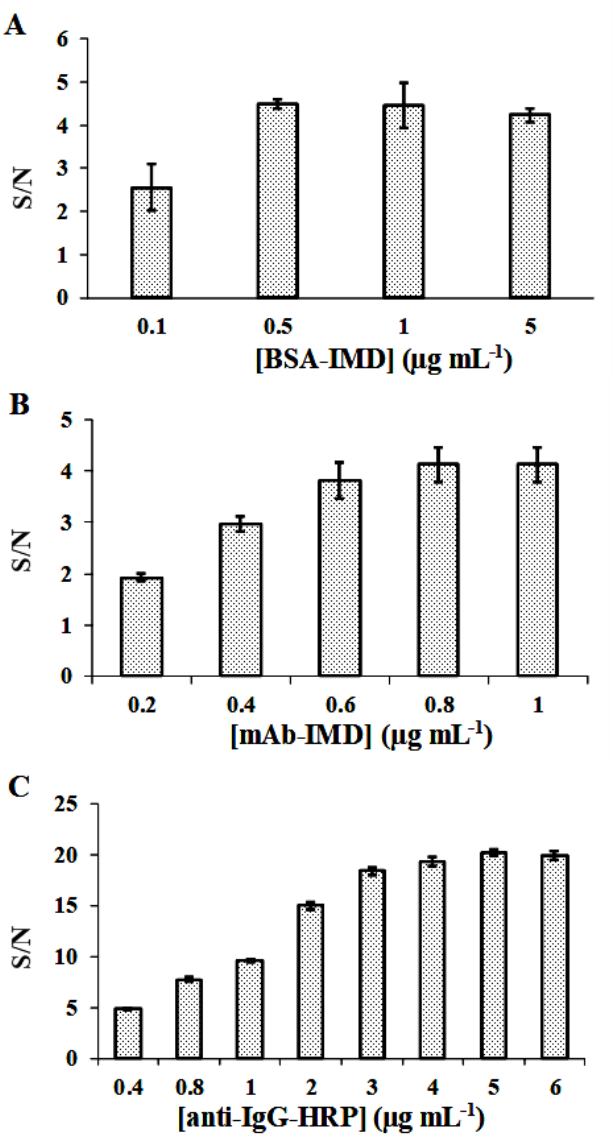

Fig. 2 Results of the optimization of: **(A)** time of enzymatic reaction, **(B)** concentration of mAb-IMD and **(C)** concentration of IMD-HRP.

3.3 Imidacloprid determination

3.3.1 Evaluation of the analytical performance of the system. Different concentrations of free IMD (50, 100, 250, 500, 750, 1000, 5000, 10000 and 20000 pM) were evaluated in the competitive immunoassay under the previously optimized conditions. Chronoamperograms displayed in Figure 3A show a decrease in the absolute value of the cathodic current

corresponding to the TMB reduction process, for increasing concentrations of IMD. The absolute value of the current generated at 60 s (response time of the sensor) was chosen as the analytical signal and used for quantification of the IMD. As shown in Figure 3B, a proportional decrease of the analytical signal was observed with corresponding increases in the

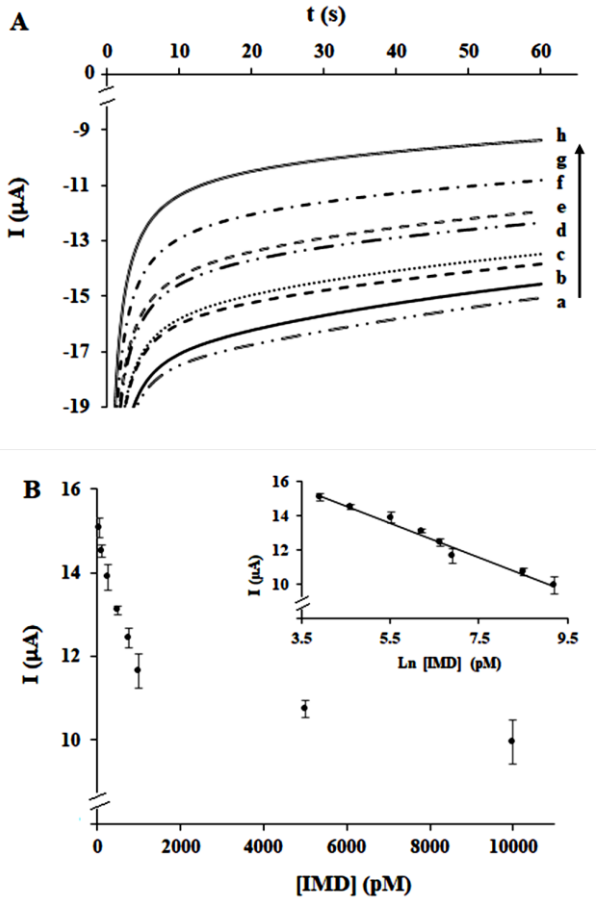

Fig. 3 (A) Chronoamperograms recorded by applying a potential of -0.2 V for 60 s, after the competitive assay performed for increasing concentrations of IMD (a) 50 pM, b) 100 pM, c) 250 pM, d) 500 pM, e) 750 pM, f) 1000 pM, g) 5000 pM, h) 10000 pM). **(B)** Relationship between the analytical signal (absolute value of current recorded at 60 s) and the IMD concentration. The logarithmic range of response is shown in the inset graph.

concentration of IMD in the range 50-10000 pM, adjusted to the following logarithmic relationship (correlation coefficient: 0.989):

$$I(\mu A) = -0.994 \mathrm{Ln}[\mathrm{IMD}](\mathrm{pM}) + 19.072$$

The limit of detection (calculated as 3Sb/m, where Sb is the deviation of the blank and m the slope of the calibration plot) was 24 pM of IMD. The reproducibility of the method shows a relative standard deviation (RSD) of 9%, obtained comparing the calibration slopes for three assays performed in different days. The inter-electrode precision was 1.9%.

HPLC-MSMS and ELISA (commercial kit) analysis were also performed for comparison purposes. Table 1 compares the analytical characteristics of the electrochemical immunosensor with those obtained with such approaches. Our device exhibits a wider linear range and lower detection limit compared to the ELISA and HPLC-MSMS methods. Furthermore, the levels reached by our immunosensor are below the maximum allowed values given by the legislation[8] (391 pM for the individual pesticides), emerging as a valid and advantageous method for the *in-situ* determination of IMD.

Table 1. Analytical characteristics for IMD detection performed with HPLC-MSMS, an ELISA kit and the electrochemical immunosensor.

Technique	Linear Range (pM)	LOD (pM)
HPLC-MSMS	391-15646	117
ELISA kit	293-4694	235
Electrochemical immunosensor	50-10000	24

Table 2. Analytical performance of different optical and electrochemical methods reported for IMD detection.

Technique	Linear Range	LOD	REF.
Electrochemical immunosensor	**50-10000 pM**	**24 pM**	**This work**
Electrochemical (BDD)	30-200 μM	9 μM	18
Electrochemical (GN/MIP/GCE)	0.5-15 μM	100 nM	19,25
Electrochemical (PCz/CRGO/GCE)	3-10 μM	440 nM	20
Electrochemical (THI/β-CD/GCE	40 nM-10 μM	17 nM	26
Electrochemical (GCE/MWCNT-f)	0.24-3.5 μM	415 nM	27
Electrochemical (PLD electro-polymerized/ TiO_2NPs/CGE)	2-400 μM	300 nM	28
Optical (ic-ELISA)	391 pM-16 nM	391 pM	29
Optical (PIF)	10 -391 nM	3 nM	30

BDD: Boron-Doped Diamond; GN: graphene; MIP: molecularly imprinted polymer; GCE: glassy carbon electrode; PCz: polycarbazole; CRGO: chemically reduced graphene oxide; THI: thionine; β-CD: β-cyclodextrin; MWCNT-f: funcionalized multi-walled carbon nanotubes; PLD: poly(levodopa); TiO_2NPs: TiO_2 nanoparticles; ic-ELISA: indirect competitive ELISA; PIF: photochemically-induced fluorimetric

Both the LOD and the linear range of response of our immunosensor are also better than those previously reported for different optical and electrochemical approaches for IMD detection, as summarized in Table 2.

Adequate controls demonstrating the suitability of the optimized biosensor format were performed. First, a pre-incubation of free IMD with the antibody, followed by incubation with the BSA-IMD on the electrode surface was evaluated. The results shown in Figure S1 at the electronic supplementary information reveal a similar sensor performance than when the simultaneous incubation is performed. This study demonstrates that such pre-incubation step is not necessary, which is advantageous for practical applications. Moreover, the response of the immunosensor in the absence of BSA-IMD and mAb-IMD was also studied. The results also

included in Figure S1 at the electronic supplementary information show that no relevant analytical signals are obtained under such conditions, evidencing the selectivity of the immunosensing response.

3.3.2 Stability and selectivity. The long-term stability of the immunosensor was evaluated by storing at 4ºC a set of electrodes with BSA-IMD immobilized. Immunoassays for an IMD concentration of 1000 pM were performed in different days for several weeks. As shown in Figure 4, the response of the immunosensor was stable and reproducible at least for 4 weeks after preparation. Longer times were not evaluated in this preliminary study.

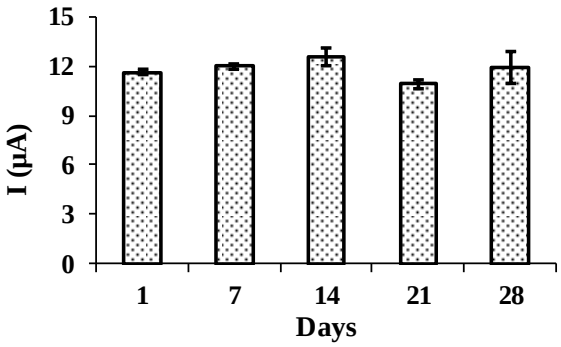

Fig. 4 Analytical signals obtained for immunoassays performed several weeks after the immunosensor preparation. IMD concentration: 1000 pM.

The selectivity of the immunosensor against other pesticides that may be present in a real sample, since as Permethrin (PERM), Glyphosate (GLY) and Parathion (PAR) was studied. Thiamethoxam (THIA) and Carbendazim (CARB) were also selected because of their chemical structure, similar than that of the IMD. Mixtures with 10000 pM of IMD and 10000 pM of the control compound were evaluated. As shown in Figure 5, no significant changes in the analytical signal were noticed for any compound, demonstrating the specificity of the immunosensor.

3.3.3 IMD analysis in real samples: evaluation of matrix effects. Spiking of IMD in tap water samples was performed to determine whether pesticide detection is affected by such real sample matrix. For the purpose, 500 pM and 1000 pM IMD solution were prepared using tap water and the results were compared with those obtained in PBS buffer. Matrix effects were calculated according the following equation[31]:

$$ME\ (\%) = (B - A\ /\ A) \times 100$$

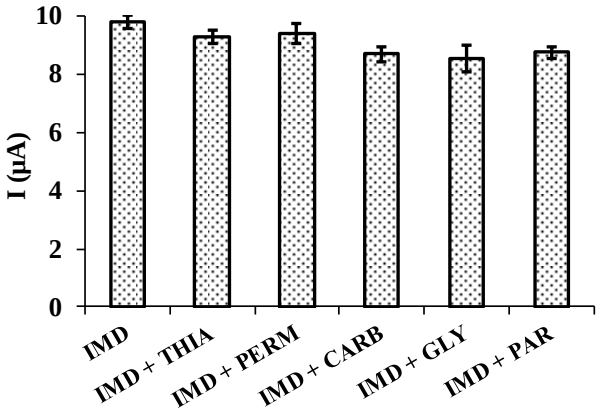

Fig. 5 Analytical signals obtained for immunoassays performed for mixtures of 10000 pM of IMD with 10000 pM of different pesticides that may be present in a real sample.

where A is the signal in buffer and B is the signal in tap water. As shown in Table 3, low matrix effects below the 6.5% were obtained, demonstrating that this technology is a reliable alternative for IMD determination in real samples.

Table 3. Evaluation of sample matrix effects. The study was done by spiking 500 pM and 1000 pM of IMD in PBS buffer and in tap water (n=4 for each sample).

Spiked IMD (pM)	Current in buffer (µA)	Current in tap water (µA)	Matrix effect
500	-13.11	-12.32	-6.4 %
1000	-11.65	-11.53	-1.0 %

4 Conclusions

Specific monoclonal antibodies have been successfully used in combination with BSA-labelled antigen and enzymatic tags for the development of a competitive immunoassay for IMD electrochemical detection. The developed immunosensor is simpler, cheaper and more rapid and sensitive than alternative standard analytical methods based on HPLC-MSMS and ELISA. The excellent performance observed in tap water samples together with the low detection limit, that is below the

maximum levels of IMD allowed by current legislation, make our approach a promising tool for the *in field* determination of this pesticide.

Conflicts of interest

"There are no conflicts to declare".

Acknowledgements

This work has been supported by the FC-15-GRUPIN-021 project from the Asturias Regional Government and the MINECO-15-CTQ2014-58826-R project from the Spanish Ministry Economy and Competitiveness (MEC). A. de la Escosura-Muñiz acknowledges the Spanish Ministry of Science, Innovation and Universities (MICINN) for the "Ramón y Cajal" Research Fellow (RyC-2016-20299).

Notes and references

1 E. Taillebois, A. Cartereau, A. K. Jones and S. H. Thany, *Pestic. Biochem. Physiol.*, 2018, 0–1.
2 C. Bass, I. Denholm, M. S. Williamson and R. Nauen, *Pestic. Biochem. Physiol.*, 2015, **121**, 78–87.
3 T. Farooqui, *Neurochem. Int.*, 2013, **62**, 122–136.
4 R. D. Booton, Y. Iwasa, J. A. R. Marshall and D. Z. Childs, *J. Theor. Biol.*, 2017, **420**, 213–219.
5 United States Environmental Protection Agency | US EPA, https://www.epa.gov/, (accessed 12 October 2018).
6 U.S. EPA, 2016, 305.
7 P. Zhang, C. Ren, H. Sun and L. Min, *Sci. Total Environ.*, 2018, **615**, 59–69.
8 Consejo de la Unión Europea, *Off. J. Eur. Communities*, 1998, **L 330**, 32–54.
9 C. Anagnostopoulos and G. E. Miliadis, *Talanta*, 2013, **112**, 1–10.
10 Z. Xiao, Y. Yang, Y. Li, X. Fan and S. Ding, *Anal. Chim. Acta*, 2013, **777**, 32–40.
11 J. L. Vilchez, R. ElKhattabi, J. Fernandez, A. GonzalezCasado and A. Navalon, *J. Chromatogr. a*, 1996, **746**, 289–294.
12 Q. Fang, L. Wang, Q. Cheng, J. Cai, Y. Wang, M. Yang, X. Hua and F. Liu, *Anal. Chim. Acta*, 2015, **881**, 82–89.
13 H. J. Kim, S. Liu, Y. S. Keum and Q. X. Li, *J Agric Food Chem*, 2003, **51**, 1823–1830.
14 E. Watanabe, K. Baba, H. Eun and S. Miyake, *Food Chem.*, 2007, **102**, 745–750.
15 S. Wanatabe, S. Ito, Y. Kamata, N. Omoda, T. Yamazaki, H. Munakata, T. Kaneko and Y. Yuasa, *Anal. Chim. Acta*, 2001, **427**, 211–219.
16 H. Lebik-elhadi, Z. Frontistis, H. Ait-amar and S. Amrani, *Process Saf. Environ. Prot.*, 2018, **116**, 535–541.
17 P. Chorti, J. Fischer, V. Vyskocil, A. Economou and J. Barek, *Electrochim. Acta*, 2014, **140**, 5–10.
18 M. Ben Brahim, H. Belhadj Ammar, R. Abdelhédi and Y. Samet, *Chinese Chem. Lett.*, 2016, **27**, 666–672.
19 M. Zhang, H. T. Zhao, T. J. Xie, X. Yang, A. J. Dong, H. Zhang, J. Wang and Z. Y. Wang, *Sensors Actuators, B Chem.*, 2017, **252**, 991–1002.
20 W. Lei, Q. Wu, W. Si, Z. Gu, Y. Zhang, J. Deng and Q. Hao, *Sensors Actuators, B Chem.*, 2013, 183.
21 F. A. Esteve-Turrillas, A. Abad-Somovilla, G. Quiñones-Reyes, C. Agulló, J. V. Mercader and A. Abad-Fuentes, *Food Chem.*, 2015, **187**, 530–536.
22 Z. Chu, J. Peng and W. Jin, *Sensors Actuators, B Chem.*, 2017, **243**, 919–926.
23 J. Biscay, M. B. G. García and A. C. García, *Sensors Actuators, B Chem.*, 2014, **205**, 426–432.
24 G. Vásquez, A. Rey, C. Rivera, C. Iregui and J. Orozco, *Biosens. Bioelectron.*, 2017, **87**, 453–458.
25 R. Li, Y. Feng, G. Pan and L. Liu, *Sensors (Basel).*, DOI:10.3390/s19010177.
26 X. Li and X. Kan, *Analyst*, 2018, **143**, 2150–2156.
27 W. D. A. Paiva, T. M. B. F. Oliveira, C. P. Sousa, P. de L. Neto, A. N. Correia, S. Morais, D. R. Silva and S. S. L. Castro, *J. Electrochem. Soc.*, 2018, **165**, B431–B435.
28 J. Ghodsi and A. A. Rafati, *Anal. Bioanal. Chem.*, 2018, **410**, 7621–7633.
29 H. J. Kim, W. L. Shelver and Q. X. Li, *Anal. Chim. Acta*, 2004, **509**, 111–118.
30 Â. L. Vilchez, R. El-khattabi, R. Blanc and A. Navalo, *Anal. Chim. Acta*, 1998, **371**, 247–253.
31 B. K. Matuszewski, M. L. Constanzer and C. M. Chavez-Eng, *Anal. Chem.*, 2003, **75**, 3019–30.

